Proceedings of the 42nd Chinese Control Conference
July 24-26, 2023, Tianjin, China

Fault Diagnosis for Robotic Fish Sensors based on Spatial Domain Image Fusion and Convolution Neural Network

Xuqing Fan[1,2], Sai Deng[1,2]*, Junfeng Fan[1,2], Chao Zhou[1,2], Zhengxing Wu[1,2], Yaming Ou[1,2], Bin Zhang[1,2]

1. The Laboratory of Cognition and Decision Intelligence for Complex Systems, Institute of Automation, Chinese Academy of Sciences, Beijing 100190

2. University of Chinese Academy of Sciences, Beijing 101408
E-mail: {fanxuqing2021,sai.deng}@ia.ac.cn

Abstract: The accurate detection of faults in robotic fish allows for improving the safety and reliability of its operations. This paper proposes a depth sensor fault diagnosis method based on Gramian Angular Field Fusion and Convolutional Neural Network (GAFF-CNN). Firstly, the depth sensor signals are augmented by a sliding window with overlapping data. Secondly, the one-dimensional time series sensor signals are converted into two-dimensional images by using Gramian Angular Field (GAF). To improve fault diagnosis accuracy and accelerate the training speed, using a weighted fusion method to fuse Gramian Angular Summation Field (GASF) and Gramian Angular Difference Field (GADF). After that, the model of CNN is established to train and test fused images for fault diagnosis. The result shows that the fault diagnosis accuracy is the highest at 97.22% when using a weighted coefficient of 0.3, and when the weighted coefficient is 0.4, the training speed is the fastest.

Key Words: Fault Diagnosis, GAF Fusion, CNN, Robotic Fish

1 Introduction

In recent years, robotic fish have attracted considerable attention from researchers and engineers due to their sufficient flexibility to swim[1]. As a branch of underwater robots, they have been used to perform complex tasks such as disaster rescue[2], ocean exploration[3], water quality monitoring[4], and so on. In order to perceive accurately and make decisions intelligently, robotic fish are equipped with a number of different types of sensors, such as depth sensors, height sensors, inertial measurement units, and so on.

However, due to the harsh working conditions and the limitations on the sensors' lifetimes, they are likely to have various faults, which can reduce the system performance and even cause safety accidents, leading to economic losses. Therefore, it is critical to diagnose sensor faults accurately to avoid accidents and improve the reliability of the robotic fish.

Various fault diagnosis methods have been proposed for fault diagnosis. In general, sensor fault diagnosis techniques can be classified into three categories: knowledge-based, model-based and data-based methods[5]. Model-based methods including state or parameter estimation methods make full use of the system model, while the utilization rate of data is not high[6]. Knowledge-based methods use expert knowledge to diagnose faults, getting rid of the dependence on accurate mathematical models[7]. Data-based methods rely on accessible data without abundant experience and huge expert knowledge, and they are suitable for systems difficult to establish explicit models or signal symptoms[8, 9].

Machine learning is one of the main methods to handle the data in data-driven fault diagnosis[10]. The traditional machine learning algorithms used consist of Support Vector Machines(SVM)[11], k-Nearest Neighbor[12], multi-layer perceptron network[13], and so on. Though they improve the accuracy of fault diagnosis, traditional machine learning methods cannot extract features automatically, resulting in time-consuming and labor-consuming because of the dependence on manual extraction. With the rapid development of machine learning, deep learning has emerged as an effective way to overcome the above drawback. Lv et al[14] proposed an end-to-end fault detection method based stacked sparse autoencoder(SAE), the method not only improved the divisibility between normal and faults data but also exhibited a better performance on the accuracy of fault classification. Mandal et al[15]used deep belief network (DBN) technology to classify the nuclear power plant thermocouple sensor fault and obtained the lowest test error compared to SVM and back propagation network.

However, the above methods only utilize the time domain features and ignore the spatial domain features. An effective method is to convert the one-dimensional time series signals into two-dimensional images. Guo et al[16] used Short Time Fourier Transform (STFT) to convert the residual signal to the corresponding time-frequency map and then designed CNN to diagnose unmanned aerial vehicle sensors' fault types. Han et al[17] used Markov Transition Field(MTF) and Gramian Angular Field(GAF) to diagnose bearing fault and obtained higher accuracy compared with other fault diagnosis methods.

To further improve the algorithm performance, Hou et al[18] proposed a spatial domain image fusion method and CNN model to locate the fault position in a nonsolid-earthed network, the input of CNN is the image fused of GASF and GADF by the given weighted coefficient 0.5, and the method achieved a great result for fault location and also provided an inspiring idea, but whether 0.5 is the optimal weighted coefficient needs further discussion. This paper transfers its regression problem of fault location to the classification problem of fault types classification. In order to obtain the best performance, the weighted fusion method is proposed for image fusion, and then explores the optimal fusion weighted coefficient.

*This work is supported by National Natural Science Foundation of China under Grant 61903362, in part by the National Natural Science Foundation of China under Grant 62003341, and in part by the Youth Innovation Promotion Association of CAS under Grant 2022130.

The main contributions of this paper are summarized as follows:

(1) The one-dimensional time series sensor signals are converted into two-dimensional images by using GAF. Then we use the weighted fusion method to fuse GASF images and GADF images to obtain GAFF images.
(2) The GAFF-CNN model is proposed by feeding the GAFF images into the CNN model to implement fault diagnosis for robotic fish depth sensor faults.
(3) Compared with the different weighted coefficients of the proposed fusion method, we find the optimal fault diagnosis performance, using fault diagnosis accuracy and model training speed as evaluation.

2 Fault diagnosis model

2.1 Data augmentation

The number of data has a great influence on diagnostic results, therefore big data to train fault diagnosis models is essential. In general, the more data, the classification effect will be better, but the training time will be longer. Hence, to strike a balance between accuracy and efficiency, the samples collected from bionic robotic fish used a sliding window with data overlap to segment the original signal into a series of equal-sized sub-signals and regard each sub-signal as one sample. In this step, a schematic diagram of data segmentation is shown in Fig. 1. Sliding window with length M slides from the start to the end of the original sample with length L. The step of the sliding window is N, and the overlap length is M-N between two samples generated by over-sampling. After obtaining sub-signals, the training and testing samples are selected according to random criteria, and the samples of each fault type are randomly assigned to the training/testing samples with a scale of 1:1.

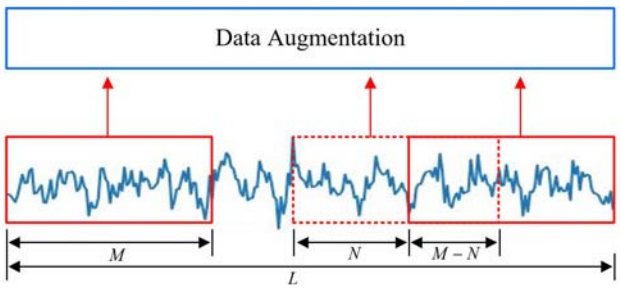

Fig. 1: Data augmentation using sliding window

2.2 Signal to image

In order to make full use of the advantages of CNN to classify fault types, GAF is used to convert one-dimensional time series sensor signals into two-dimensional images, which is shown in Fig. 2. The basic idea is to take one-dimensional time series signals in cartesian coordinate system, transform them into polar coordinate system representations, and then use trigonometric functions to generate a GAF matrix. The time series noise is eliminated by spatial transformation and the vector inner product is used to preserve the time information. According to the different calculation methods of the GAF matrix formed, there can be divided into two categories, one is the cosine of the summed angles for GASF and the other is the sine of the subtracted angles for the GADF. This is explained mathematically as follows.

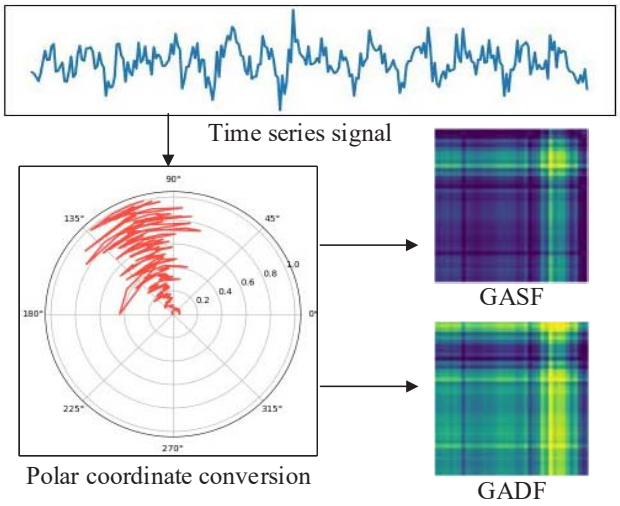

Fig. 2: The method of signal to GASF and GADF image

The first step is to normalize the time series signals to the interval [-1,1], assuming that one of time series signals is $X = x_1, x_2, \ldots, x_N$, and the normalized value $\tilde{x}_i$ can be calculated by

$$\tilde{x}_i = \frac{x_i - \max(X) + (x_i - \min(X))}{\max(X) - \min(X)} \tag{1}$$

Then we can represent the rescaled time series $\tilde{X}$ in polar coordinates by encoding the value as the angular cosine and the time stamp as the radius with the equation below:

$$\begin{cases} \phi_i = \arccos\left(\tilde{x}_i\right), -1 \le \tilde{x}_i \le 1, \tilde{x}_i \in \tilde{X} \\ r_i = \dfrac{t_i}{n}, t_i \in \mathbb{N} \end{cases} \tag{2}$$

In the equation above, ϕ_i is the polar angle fall in the angle boundaries $[0, \pi]$, r_i represents the radius of the polar coordinate, t_i is the time stamp, and n is a constant factor to regularize the span of the polar coordinate system.

After the time series signals has been transformed within polar coordinates, each point is represented as the radius and angle. the next step is to mine the correlation between different moment points by the angle of each moment point, the GASF can be generated by the cosine of the summed angles as follows:

$$\text{GASF} = \begin{pmatrix} \cos(\phi_1 + \phi_1) & \cdots & \cos(\phi_1 + \phi_n) \\ \cos(\phi_2 + \phi_1) & \cdots & \cos(\phi_2 + \phi_n) \\ \vdots & \vdots & \vdots \\ \vdots & \vdots & \vdots \\ \cos(\phi_n + \phi_1) & \cdots & \cos(\phi_n + \phi_n) \end{pmatrix} = \tilde{X}^T \cdot \tilde{X} - \sqrt{I - \tilde{X}^2}^T \cdot \sqrt{I - \tilde{X}^2} \tag{3}$$

The GADF algorithm is similar to the GASF except that GADF is constructed using the sine of the subtracted angles as follows:

$$\text{GADF}=\begin{pmatrix} \sin(\phi_1-\phi_1) & \cdots & \sin(\phi_1-\phi_n) \\ \sin(\phi_2-\phi_1) & \cdots & \sin(\phi_2-\phi_n) \\ \vdots & \vdots & \vdots \\ \vdots & \vdots & \vdots \\ \sin(\phi_n-\phi_1) & \cdots & \sin(\phi_n-\phi_n) \end{pmatrix} = \sqrt{I-\tilde{X}^2}\cdot\tilde{X}-\tilde{X}^T\cdot\sqrt{I-\tilde{X}^2}\cdot \quad (4)$$

The method of signal-image conversion has two major advantages as follows:

(1) The relationship between the one-dimensional time series sensor signals and the two-dimensional images is double-mapping relation, which does not lose any information about the one-dimensional time series sensor signals.

(2) It can maintain the time dependence of signals. The texture information and color distribution of the two-dimensional images can reflect the invisible information of the one-dimensional time series sensor signals [18].

2.3 Weighted fusion method for GAF

Since the signal can be converted into GASF and GADF images, for the purpose of taking advantage of both, weighted fusion method is used to generate the GAFF images as equation (5) shows. It is a transparency fusion method that is widely used in image composition and image matting fields.

$$GAFF = \alpha * GASF + (1-\alpha) * GADF \quad (5)$$

GASF image is the foreground image and its transparency denotes as α, GADF image is the background image and its transparency is $1-\alpha$, where the value range of α is[0,1], the process to fuse each image pixel with $\alpha = 0.5$ is shown in Fig. 3, GAFF image has both GASF's and GADF's information. When α is 0, GAFF image only has GASF's information; And when α is 1, GAFF image only has GADF's information. With adjustable weighted coefficient α, we can generate different images to find the optimal fault diagnosis performance.

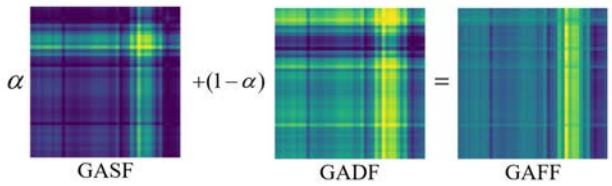

Fig. 3: Weighted fusion method for GAF

2.4 Convolutional Neural Network Structure

Once the raw signals have been converted into GAFF images, CNN can be trained to classify these images. CNN is a multilayer supervised learning neural network, and the convolutional and pool sampling layers of the implicit layer are the core modules to realize the feature extraction function of CNN. The network model improves the accuracy of the network through frequent iterative training by minimizing the loss function using the gradient descent method to adjust the weighted coefficient in the network layer by layer in reverse.

The low hidden layer of the CNN is composed of alternating convolutional layer and maximum pool sampling layer, and the high level is a fully connected layer corresponding to the implicit layer of a traditional multilayer perceptron and a logistic regression classifier. The input of the first fully connected layer is a featured image obtained by feature extraction from the convolutional and subsampling layers, and the final output layer is a classifier layer that can classify the input images using the softmax function to achieve logistic regression. There are four key ideas behind CNN that take advantage of the properties of natural signals: local connections, shared weights, pooling, and the use of many layers.

In order to classify the fault types, A CNN structure with three convolutional layers is designed to diagnose robotic fish sensor faults as shown in Fig. 4. It is an end-to-end model which doesn't need manual feature extraction, what we need is to select inputs and outputs.

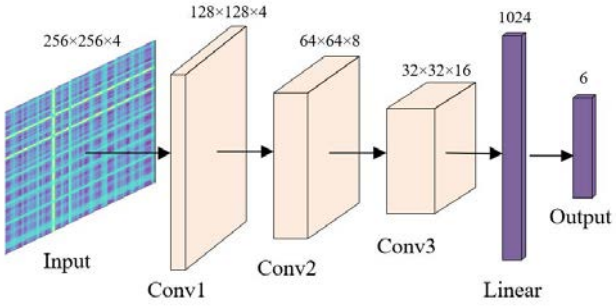

Fig. 4:The structure of CNN

GAFF images are inputted to CNN with a batch, and the dimensionalities of each image are (256,256). Firstly, GAFF images are convoluted by (5,5) kernel and activated by the ReLU function, then go through a max pooling process to reduce features maps' dimensionalities. Secondly, features images perform two consecutive convolutions and max pooling to obtain the deeper and the more abstract features with the same convolutional kernel of (3×3). Thirdly, in order to classify images, the feature maps are flattened to a vector and then performed a linear connection to obtain a feature vector. Finally, the feature vector is connected with the output layer using the softmax function to achieve fault classification.

3 Verification

3.1 Experimental data collection

As illustrated in Fig. 5, the robotic fish is comprised of a pair of pectoral fins, and a three-link posterior body with a caudal fin. To obtain better underwater kinematic ability, an embedded control system based on STM32F407 microcontroller is built. The microcontroller is used to drive the robotic fish and Central Pattern Generator (CPG) governed control strategy is adopted to realize various sharklike motions[19]. It is powered by batteries, which increases the flexibility of movement by eliminating the dependence on cables. In order to achieve intelligent perception and precise control, it is equipped with Inertial Measurement Unit (IMU), depth sensor, and infrared sensor.

The depth sensor is on the surface of the fish body, so it has a greater risk of failure due to collision with the environment compared to the IMU and the infrared sensor inside the body of the robotic fish. Therefore, this paper focuses on the fault diagnosis of depth sensor.

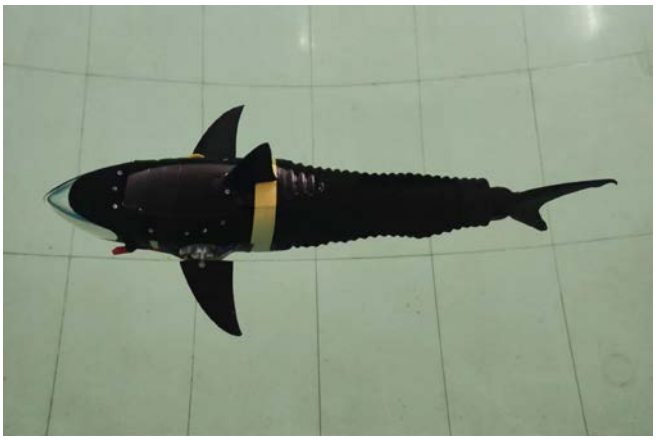

Fig. 5 Photograph of the robotic prototype

In order to verify the effectiveness of the proposed GAFF-CNN based fault diagnosis for the robotic fish, aquatic experiments were carried out in a lab pool, whose dimensions are 500 cm × 400 cm × 120 cm, as shown in Fig. 6. In order to collect information about the robotic shark, a data collection system based on HC-12 was designed. HC-12 is a wireless communication module operating in the 433 MHz bands. Not only does it operate at a low frequency, but also has a high transmitting power, so it is ideal for communicating with the robotic shark. A data collection software was developed in the host PC and the process of data collection is as follows. Firstly, the host PC sends control commands and the robotic shark starts to move following the command, the host PC is sending port and the robotic shark is receiving port during this process. Meanwhile, the robotic shark records sensor information to an SD card, which can be recorded in real-time. Finally, the host PC receives sensor data from the robotic shark and records it in the database, the robotic shark is sending port and the host PC is receiving port in this process.

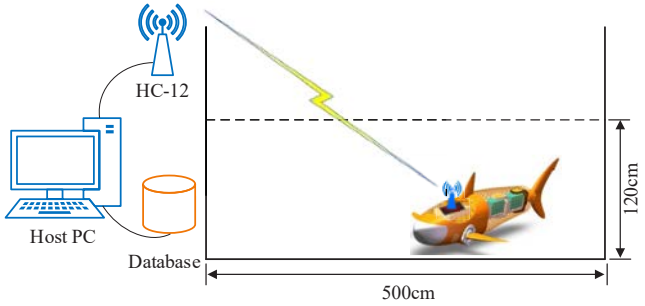

Fig. 6: Schematic diagram of data collection

In experiments, six depth sensor types were collected including the Normal type and five fault types: No Output type, Drift type, Interrupt type, Constant type, and Jump type as shown in Fig. 7. At the beginning, the robot fish was in normal operation, after a period of normal operation, the sensor faults occurred, which caused chain reactions and curve fluctuations. In order to reduce the impact of different tasks of robotic fish on sensor fault diagnosis, the data of the curve is the sensor's depth value subtracted by the target depth value. As we can see, the curve of the Interrupt fault and the Jump fault is similar, and the curve of the Normal type and the Drift type have similar fluctuation shapes, which increases the difficulty of fault diagnosis.

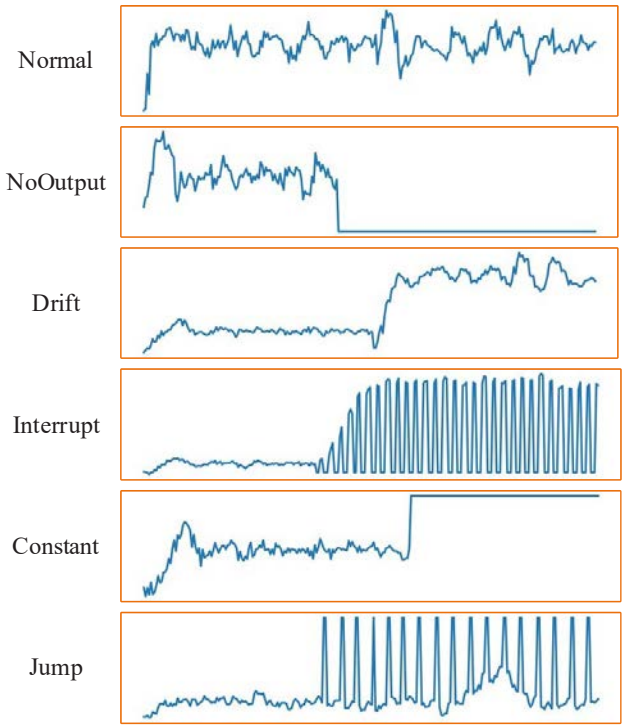

Fig. 7 Depth sensor data

To ensure the robustness of the model and to remove the influence of outliers on the accuracy of the model, the signals were normalized to between [0,1], and in order to avoid the impact of unbalanced data on the different fault types, the same amount of data of each type was selected among the collected data.

3.2 GAFF image generation

The data collected from robotic fish were time series signals, which can be converted into GASF and GADF images. To take advantage of both, weighted fusion method was used to generate GAFF images as shown in Fig. 8. The sub-signals' length is 256, so the image dimensionalities of GAFF are (256,256). At each pixel point, where both GASF and GADF are bright, GAFF is enhanced, increasing the degree of feature differentiation; for pixels where GASF is relatively bright and GADF is relatively not bright, or both are opposite, the brightness is balanced to reduce the possibility of false recognition.

As we can see, there are many textural features in GAFF images, the distinguishing degree of different state type features is obvious, which lays the foundation for CNN to classify. The original number of each type was 20, for the purpose of improving the training stability, the sliding window method was adopted to increase the number of each type to 200. As for the input of CNN, to make the convergence more stable and efficient, GAFF images were input with the batch size of 4.

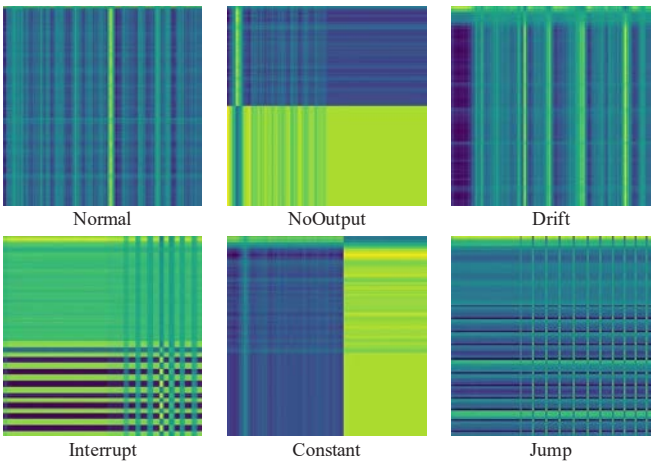

Fig. 8: GAFF images

3.3 Result of fault diagnosis

The confusion matrix, also known as the error matrix, is a common format for representing the classification evaluation of a model, and it enables and it enables visualization of the accuracy of correct classification for each class. Fig. 9 presents the best confusion matrix of the result of GAFF-CNN When transparency α is 0.3, which obtains the total prediction accuracy of 97.22%. The rows stand for the true label, and the columns stand for the predicted label for each condition. The Normal and the Jump type are all correctly classified, and the rest have a low rate of misidentification, it is a possible reason that the Normal and the Jump type both have relatively distinct texture features compared to others.

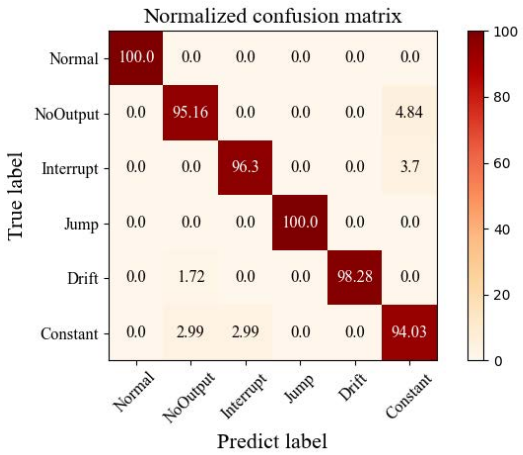

Fig. 9: Confusion matrix of the result

Furthermore, for the visual study of the diagnosis effect, the T-Distributed Stochastic Neighbor embedding(T-SNE) algorithm was used to reduce the dimensionality of the last layer feature of CNN. It is a nonlinear dimensionality reduction algorithm, which is very suitable for the dimensionality reduction of high-dimensional data to two or three dimensions for visualization, and the ideal classification is that similar data is close, and dissimilar data is far away. In order to visually saw the result, we used a scatter diagram to display the last layer's classification results, as shown in Fig. 10.

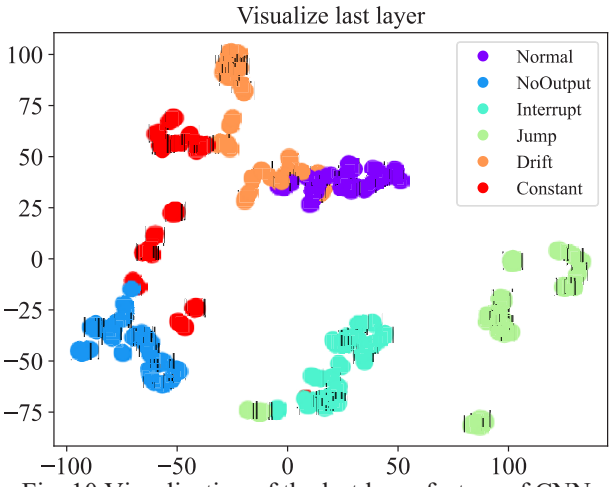

Fig. 10 Visualization of the last layer feature of CNN

In Fig. 10, the Constant fault type distribution is relatively scattered, which has the lowest accuracy 94.03%. Though the Normal type and the Drift fault type have many overlaps, they are correctly classified by the softmax function, one possible reason is that T-SNE is a dimensionality reduction method, and its essence is a projection, which has distortion from high dimension to low dimension.

3.4 Comparative analysis

As for the same structure and parameters of CNN, the factor that influences the accuracy of fault diagnosis is the input image. For image fusion, the weighted coefficient of transparency between the foreground and background has a great impact on the fused image, which in turn affects the effectiveness of fault diagnosis. Accuracy and error curves were obtained by changing the value of the weighted coefficient α as shown in Fig. 11. GAFF-CNN has the highest accuracy of 97.22% when α is 0.3, and the lowest accuracy of 91.67% when α is 0.9.

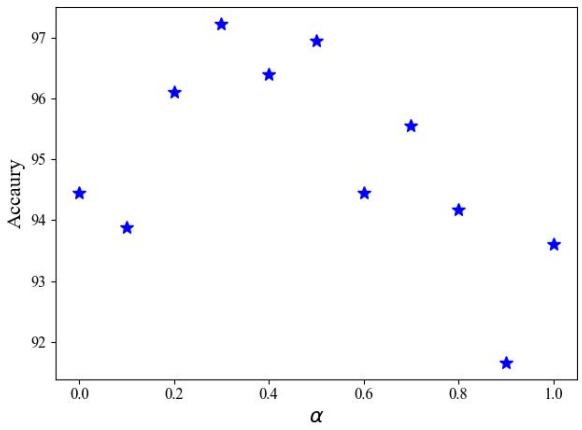

Fig. 11: The prediction accuracy with various α

Furthermore, we not only considered diagnosis accuracy but also cared for convergence speed, so loss curves were plotted to explore the convergence between different weighted coefficients. As shown in Fig. 12, when the weighted coefficient α is 0.4, the loss curve drops fastest and converges to the minimum earliest in the 20th epoch, but the accuracy is not the highest. Therefore, it is a contradiction that needs to be balanced between diagnosis accuracy and

convergence speed when expanding the application of this method.

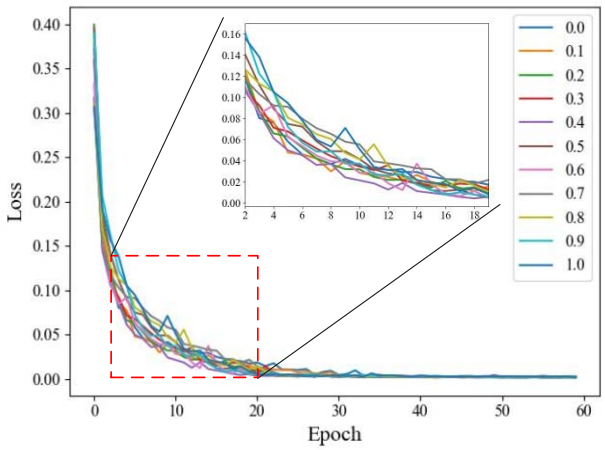

Fig. 12: The loss curves with various α

The comparative analysis showed that the GAFF-CNN method proposed in our work has great advantages in robotic fish depth sensor fault diagnosis, and the variable weighted coefficient has an important impact on both diagnosis accuracy and convergence speed, which we can acquire the optimal performance by optimizing it.

4 Conclusion

This study proposes a GAFF-CNN intelligent diagnosis method for robotic fish sensor faults. The main contributions of this study are summarized as: (i) The one-dimensional time series sensor signals are converted into two-dimensional images by using GAF; (ii) GASF and GADF images are fused by weighted fusion method to generate GAFF image, and the CNN diagnosis model is designed. (iii)Weighted coefficients of GAF fusion are explored, showing that it has an important impact on both diagnosis accuracy and convergence speed. These results show the great potential of the proposed GAFF-CNN method in the data-driven fault diagnosis field.

References

[1] Y. Yang, J. Wang, Z. Wu, et al., Fault-tolerant control of a CPG-governed robotic fish, Engineering, 4(6): 861-868, 2018.

[2] J. Yu, L. Wang, J. Shao, et al., Control and coordination of multiple biomimetic robotic fish, IEEE transactions on control systems technology, 15(1): 176-183, 2006.

[3] G. Li, X. Chen, F. Zhou, et al., Self-powered soft robot in the Mariana Trench, Nature, 591(7848): 66-71, 2021.

[4] Z. Wu, J. Liu, J. Yu, et al., Development of a novel robotic dolphin and its application to water quality monitoring, IEEE/ASME Transactions on Mechatronics, 22(5): 2130-2140, 2017.

[5] H. Wu and J. Zhao, Deep convolutional neural network model based chemical process fault diagnosis, Computers & chemical engineering, 115: 185-197, 2018.

[6] X. Yan, T. Sheng, X. Xie, et al., Convolutional Neural Network-based Fault Diagnosis for Spacecraft Attitude Multiple Components, 41st Chinese Control Conference (CCC), 2022: 3935-3941.

[7] Z. Dong, J. Zhao, J. Duan, et al., Research on agricultural machinery fault diagnosis system based on expert system, 2nd IEEE Advanced Information Management, Communicates, Electronic and Automation Control Conference (IMCEC), 2018: 2057-2060.

[8] Y. Lei, B. Yang, X. Jiang, et al., Applications of machine learning to machine fault diagnosis: A review and roadmap, Mechanical Systems and Signal Processing, 138: 106587, 2020.

[9] A. Slimani, P. Ribot, E. Chanthery, et al., Fusion of model-based and data-based fault diagnosis approaches, IFAC-PapersOnLine, 51(24): 1205-1211, 2018.

[10] L. Wen, X. Li, L. Gao, et al., A New Convolutional Neural Network-Based Data-Driven Fault Diagnosis Method, IEEE Transactions on Industrial Electronics, 2017.

[11] C. Li, R.-V. Sanchez, G. Zurita, et al., Multimodal deep support vector classification with homologous features and its application to gearbox fault diagnosis, Neurocomputing, 168: 119-127, 2015.

[12] Q. P. He and J. Wang, Fault detection using the k-nearest neighbor rule for semiconductor manufacturing processes, IEEE transactions on semiconductor manufacturing, 20(4): 345-354, 2007.

[13] S. S. Tayarani-Bathaie, Z. S. Vanini and K. Khorasani, Dynamic neural network-based fault diagnosis of gas turbine engines, Neurocomputing, 125: 153-165, 2014.

[14] F. Lv, C. Wen, Z. Bao, et al., Fault diagnosis based on deep learning, 2016 American control conference (ACC), 2016: 6851-6856.

[15] S. Mandal, B. Santhi, S. Sridhar, et al., Nuclear power plant thermocouple sensor-fault detection and classification using deep learning and generalized likelihood ratio test, IEEE Transactions on nuclear science, 64(6): 1526-1534, 2017.

[16] D. Guo, M. Zhong, H. Ji, et al., A hybrid feature model and deep learning based fault diagnosis for unmanned aerial vehicle sensors, Neurocomputing, 319: 155-163, 2018.

[17] B. Han, H. Zhang, M. Sun, et al., A new bearing fault diagnosis method based on capsule network and markov transition field/gramian angular field, Sensors, 21(22): 7762, 2021.

[18] S. Hou and W. Guo, Fault Location Method in Nonsolid-Earthed Network Based on Spatial Domain Image Fusion and Convolution Neural Network, Journal of Sensors, 2022.

[19] X. Yang, Z. Wu and J. Yu, Design and implementation of a robotic shark with a novel embedded vision system, IEEE International Conference on Robotics and Biomimetics (ROBIO), 2016: 841-846.